29 p.

NASA TECHNICAL MEMORANDUM

NASA TM X-889

NASA TM X-889

WIND-TUNNEL INVESTIGATION OF THE SONIC-BOOM CHARACTERISTICS OF THREE PROPOSED SUPERSONIC TRANSPORT CONFIGURATIONS

by Harry W. Carlson and Barrett L. Shrout
Langley Research Center
Langley Station, Hampton, Va.

NATIONAL AERONAUTICS AND SPACE ADMINISTRATION WASHINGTON, D.C. OCTOBER 1963

TECHNICAL MEMORANDUM X-889

WIND-TUNNEL INVESTIGATION OF THE SONIC-BOOM CHARACTERISTICS OF THREE PROPOSED SUPERSONIC TRANSPORT CONFIGURATIONS

By Harry W. Carlson and Barrett L. Shrout

Langley Research Center
Langley Station, Hampton, Va.

NATIONAL AERONAUTICS AND SPACE ADMINISTRATION

NATIONAL AERONAUTICS AND SPACE ADMINISTRATION

TECHNICAL MEMORANDUM X-889

WIND-TUNNEL INVESTIGATION OF THE SONIC-BOOM CHARACTERISTICS OF THREE PROPOSED SUPERSONIC TRANSPORT CONFIGURATIONS*

By Harry W. Carlson and Barrett L. Shrout

SUMMARY

Wind-tunnel measurements of the sonic-boom pressure signatures of models of three proposed supersonic transports have been made in the Langley 4- by 4-foot supersonic pressure tunnel. The results have shown reasonable correlation of adjusted pressure rise values with available theory, observed discrepancies being at most 10 percent of the measured values of overpressures. Estimated ground overpressures for airplanes with equal weights of 300,000 pounds at a representative cruise altitude of 70,000 feet range from 1.4 lb/sq ft for a highly swept arrow-wing configuration to 1.65 lb/sq ft for a configuration employing a wing of moderate sweep in an aft location.

INTRODUCTION

Sonic-boom considerations are certain to have a large influence on the operational procedures adopted for future supersonic air transports. This noise problem may also to some degree influence the choice of airplane configuration.

The purpose of this investigation is to establish in general the magnitude of the ground overpressures and to provide information relative to the dependence of boom strength on configuration. Measurements of the sonic-boom pressure signatures of three supersonic transport configurations have been made in a series of tests conducted in the Langley 4- by 4-foot supersonic pressure tunnel. The models are very small scale representations of the configurations whose aerodynamic characteristics were studied in references 1, 2, and 3. The tests at Mach numbers of 1.41 and 2.01 were performed by using the apparatus and techniques described in reference 4. Both wind-tunnel measurements and available theory have been used in making estimates of overpressure on the ground for supersonic-transport cruise conditions.

SYMBOLS

A	cross-sectional area of configuration
$A\left(\frac{t}{L}\right)$	nondimensionalized cross-sectional area, $\frac{A}{L^2}$
$B\left(\frac{t}{L}\right)$	nondimensionalized lift distribution function given by $B\left(\frac{t}{L}\right) = \frac{1}{L^2}\int_0^t \frac{l}{q}\,dt$
C_L	lift coefficient
$C_{L,o}$	lift coefficient at zero angle of attack
C_{L_α}	lift-curve slope
K_l	reflection factor
L	length of models or of airplane
l	lift per unit length along airplane axis
M	Mach number
p	reference pressure, free-stream static pressure for tunnel tests and pressure at mid-altitude for flight estimates (mid-altitude is altitude of point halfway between ground and airplane)
Δp	incremental pressure above or below the ambient pressure due to flow field of airplane or model
Δp_{max}	maximum value of Δp at bow shock
$\left(\frac{\Delta p}{p}\right)_{max}$	maximum pressure ratio at bow shock
q	free-stream dynamic pressure
S	wing area
t,τ	dummy variables of integration, measured in same direction and using same units as x
V	volume of airplane
W	weight of airplane

X,Y Cartesian coordinates of field point, X measured in free-stream direction and Y measured normal to free-stream direction positive downward

ΔX distance from point on pressure signature to point where pressure signature curve crosses zero pressure reference axis

δX change in position of bow shock due to vibration

x distance from nose measured along airplane or model axis

$\beta = \sqrt{M^2 - 1}$

γ ratio of specific heats for air, 1.4

A double prime (") denotes a second derivative with respect to distance.

MODELS AND TESTS

Photographs and drawings of the test models are shown in figures 1 and 2, respectively. The following table gives for each configuration the reference from which the model geometry was derived, the scale relative to that of the references, the sonic-boom-model assumed length, and nondimensional values of wing areas and total volumes.

Configuration	Reference	Scale	L, in.	S/L^2	V/L^3
1	1	0.0211	1.02	0.126	0.00255
2	2	.0250	1.15	.097	.00258
3	3	.0244	1.0	.113	.00328

These small models duplicated most but not all of the major features of the proposed transport configurations. Configuration 1 was built without the fuselage camber of the original. In configuration 2, the empennage and nacelles have been omitted, but the nacelle volume was accounted for in a thickened wing trailing edge. Configuration 3 is essentially complete but has minor changes in fuselage camber. In designing the models, the engine-stream-tube capture area has been subtracted from the nacelle or engine package cross-sectional area.

The lift-coefficient variation with angle of attack has been estimated from the aerodynamic data of references 1, 2, and 3 by taking into account insofar as possible the previously mentioned departures of the sonic-boom models from the force models. This information is summarized in the following table:

Configuration	M = 1.41		M = 2.01	
	$C_{L,o}$	C_{L_α}	$C_{L,o}$	C_{L_α}
1	0.016	0.034	0.014	0.029
2	.067	.040	.053	.034
3	.019	.069	.014	.047

The lift coefficient for each test condition was calculated by using these estimates taking into account measured tunnel flow angularity, and deflections of the models under load.

The tests were conducted in the Langley 4- by 4-foot supersonic pressure tunnel at Mach numbers of 2.01 and 1.41 and a Reynolds number per foot of 2.5×10^6. A sketch of the test apparatus is shown in figure 3. The model was sting mounted on a support system which provided for remotely controlled adjustments in the longitudinal position of the model. Measurements of the pressure field were made by means of static-pressure probes located at distances measured perpendicular to the free-stream direction of 12.5, 25, and 50 inches from the model at M = 2.01 and of 12.5, 25, and 42 inches from the model at M = 1.41. The probes were very slender cones (1° cone angle) with four 0.013-inch-diameter static-pressure orifices leading to a common chamber. The orifices were circumferentially spaced 90° apart and were arranged to lie in a Mach cone originating at the model. Models were mounted in the tunnel in inverted positions so that the measured pressure signatures would correspond to those found directly below an airplane in normal-flight attitude.

THEORETICAL CONSIDERATIONS

An expression derived from reference 5 gives the pressure rise at the bow shock emanating from a wing-body combination in a uniform atmosphere as:

$$\left(\frac{\Delta p}{p}\right)_{max}\left(\frac{Y}{L}\right)^{3/4} = K_1 \beta^{1/4} \frac{1.19\gamma}{\sqrt{\gamma + 1}} \sqrt{\int_0^{T_0} F\left(\frac{\tau}{L}\right) d\left(\frac{\tau}{L}\right)} \qquad (1)$$

The term K_1 is a reflection factor which depends on the nature of the surface on which the measurements are made. For the measuring probes used in these tests a reflection factor of unity was assumed. The limit T_0 is the root of the equation $F\left(\frac{\tau}{L}\right) = 0$ which gives the largest positive value for the integral.

The function $F\left(\frac{\tau}{L}\right)$ depends on the longitudinal distribution of cross-sectional area and of lift as defined in the following equation:

$$F\left(\frac{\tau}{L}\right) = \frac{1}{2\pi} \int_0^{\tau/L} \frac{A''\left(\frac{t}{L}\right)}{\sqrt{\frac{\tau}{L} - \frac{t}{L}}} d\left(\frac{t}{L}\right) + \frac{\beta}{4\pi} \int_0^{\tau/L} \frac{B''\left(\frac{t}{L}\right)}{\sqrt{\frac{\tau}{L} - \frac{t}{L}}} d\left(\frac{t}{L}\right) \qquad (2)$$

The area distribution of the models shown in figure 2 represents normal cross-sectional areas corresponding to $M = 1.0$ supersonic area rule cuts. In the interest of simplicity, a uniform distribution of lift over the wing planform was assumed to exist. The equations were evaluated in a manner similar to that used in reference 6. The calculation procedures were adapted to machine computing, 40 points along the body axis being used to describe the area and lift distributions.

The length of the positive portion of the pressure signature can be expressed by the following equation derived from reference 5:

$$\frac{\Delta X}{L}\left(\frac{Y}{L}\right)^{-1/4} = 1.19 \frac{(\gamma + 1)}{\sqrt{\gamma + 1}} \frac{M^2}{\beta^{3/4}} \sqrt{\int_0^{T_0} F\left(\frac{\tau}{L}\right) d\left(\frac{\tau}{L}\right)} \qquad (3)$$

The slope of the linear portion of the signature may thus be written in the following form which shows its independence of airplane geometry:

$$\frac{\Delta p}{\Delta X} = K_1 \frac{p}{Y} \frac{\beta}{M^2} \frac{\gamma}{\gamma + 1}$$

RESULTS AND DISCUSSION

Measurements of pressure signatures for the three configurations are shown in figure 4. Pressures and distances are plotted in parametric form in accordance with theoretical considerations. (See eqs. (1) and (3).) According to theory, the far-field pressure signatures for a given model and lifting condition when plotted in this form should be identical regardless of distance and should assume a characteristic "N" shape. In some cases it is quite evident that this far-field condition has not been attained. Failure to display the N-shape is more noticeable at the lower lift coefficients, particularly at $M = 1.41$.

In order to compensate for the lack of attainment of far-field conditions, for the probe boundary layer, and for the effects of vibration of the models and test apparatus, the maximum pressure-rise ratio at the bow shock was found by using the method discussed in the appendix of this report. This adjusted value of the bow-shock pressure rise has been plotted against distance in figure 5. The faired curves of these plots represent an attempt at extrapolation to the eventual constant value of the parameter as far-field conditions are approached.

Extrapolated tunnel sonic-boom data are compared with theory in figure 6. A pressure-rise parameter has been plotted against a lift parameter. These

parameters permit data for all Mach numbers and lift coefficients to be plotted on a single set of axes. The cross-hatched band represents a fairing of the experimental data. Theoretical estimates are shown as two curves: for one, boundary-layer effects on the model are ignored; for the other, the area distribution used in the calculations includes the estimated area contained within the displacement thickness of a laminar boundary layer. An improved correlation may be noted when boundary-layer effects are included. The greatest discrepancies between theory and experiment occur for configuration 1, where the measured overpressures are some 6 to 10 percent greater than indicated by the theory. The reason for this discrepancy contrasted with the good agreement for configurations 2 and 3 has not been determined. The magnitude of the difference in overpressure is slightly greater than that which would be caused by the presence of a turbulent boundary layer on the model rather than the assumed laminar layer. In comparing the overpressure parameters for the three configurations it is of interest to note that configurations 1 and 2 which more nearly meet the requirements for an approach to the sonic-boom lower bound as discussed in reference 7, do in fact have lower measured values of the parameter. In view of the difficulties associated with the construction and testing of these extremely small models and in ascertaining how closely the completed model followed the model drawings, there is some question whether the experimental data or the theory will provide the more accurate estimate of the sonic-boom characteristics of these configurations.

Estimates of the overpressure on the ground to be expected during flight may be made with the use of both theory and wind-tunnel data. In the estimates shown in figure 7 a weight of 360,000 pounds at a Mach number of 1.41 was chosen to represent the climb-out portion of the flight and a weight of 300,000 pounds at a Mach number of 3.0 was chosen to represent the cruise portion. The length was chosen so that each configuration would have a total volume of 15,000 cu ft. Estimates of ground overpressures based on the adjusted wind-tunnel measurements of bow-shock pressure rise take into account differences between effective area distribution of models and full-size airplanes due to differences in the displacement thickness of the boundary layer as discussed in the example given in the appendix. A reference pressure p equal to the atmospheric pressure at mid-altitude was used since in reference 4 this method gave good correlation of tunnel data and flight data from reference 8. (A rigorous treatment of the effects of a nonuniform atmosphere may be found in ref. 9.) It is necessary to establish a reflection factor since overpressure at ground level depends directly on its value. The factor of 2.0 found to apply for the dry lake bed over which the flight tests of reference 8 were conducted may not be representative of average conditions over the continental United States; however, an overall average is likely to be greater than the factor of 1.75 to 1.80 measured in reference 10. A compromise value of 1.9 was chosen for use in the present study. Overpressure estimates for a representative cruise altitude of 70,000 feet range from a value of about 1.4 lb/sq ft for configuration 2 to about 1.65 lb/sq ft for configuration 3. It must be understood that these overpressure values depend on the assumed weights which may not be quite realistic and furthermore are not likely to be equal for actual airplanes based on the several configurations necessary to fulfill the same mission requirements.

CONCLUDING REMARKS

Wind-tunnel measurements of the sonic-boom characteristics of three supersonic transport configurations have shown reasonable correlation of adjusted pressure-rise values with available theory, observed discrepancies being at most 10 percent of the measured values of overpressures. Estimated ground overpressures for airplanes with equal weights of 300,000 pounds at a representative cruise attitude of 70,000 feet range from about 1.4 lb/sq ft for a highly swept arrow-wing configuration to about 1.65 lb/sq ft for a configuration employing a wing of moderate sweep in an aft location.

Langley Research Center,
National Aeronautics and Space Administration,
Langley Station, Hampton, Va., June 20, 1963.

[redacted]

APPENDIX

ADJUSTMENTS OF WIND-TUNNEL MEASUREMENTS OF BOW-SHOCK STRENGTH TO COMPENSATE FOR EXPERIMENTAL DEFICIENCIES

A number of experimental difficulties arise in attempting to measure within the confines of a wind tunnel the pressure signatures of the necessarily small models and in attempting to extend the results to apply to full-size airplanes at flight altitudes. The necessity of attaining or approaching far-field conditions where the pressure signature assumes a characteristic N-shape requires that tunnel models be extremely small. Even with models as small as those employed in the present investigation the failure to achieve in all cases an approach to far-field conditions creates serious problems. It does not appear to be practical to reduce further the model size because of construction difficulties and because vibrations of models, probes, and support apparatus introduce changes in the shape of the pressure signature and in the magnitude of the pressure rise, which become progressively more pronounced as model size is decreased. The presence of a boundary layer on the measuring probe also introduces changes in the shape of the signature and in the magnitude of the pressure rise, which are dependent on model size. Another result of decreased model size is the increase in relative importance of the increment in effective cross-sectional area due to model boundary layer discussed in the text.

With a compromise model size the experimental deficiencies in attaining a far-field N pressure signature are always present to some degree and are sometimes large. Thus, a method of interpreting the results and compensating for these deficiencies becomes necessary. The following discussion explores these problems and suggests a method of adjusting the wind-tunnel data.

The failure to achieve a classical N-wave in the present tests is due in part to the fact that in many cases the pressure signatures are in the transition region from near-field to far-field conditions. The near-field shape of the pressure signature is evidenced by the presence of two distinct pulses in the region of the bow shock. These probably are the separate shocks from the fuselage nose and from the wing-body juncture. It has been noted that, even for quite complex signatures, a linear portion of the pressure signature develops and the slope closely agrees with the estimated one when far-field theory is used. By accepting the premise that, during this transition, the impulse area under the bow shock portion of the signature attenuates with distance in a manner identical to that for a fully developed N-wave, an attempt may be made to define the pressure signature that would exist if far-field conditions were established. The adjusted signature may be determined as illustrated in sketch 1 simply by extending the linear portion of the measured signature forward so that a right triangle is formed whose area is equal to the area under the measured curve. Because of inexactness in the assumptions, the adjustment cannot be rigorously correct; however, a practical test would appear to be met when adjusted signatures plotted in the form used in figure 4 remain constant as distance is increased.

[redacted]

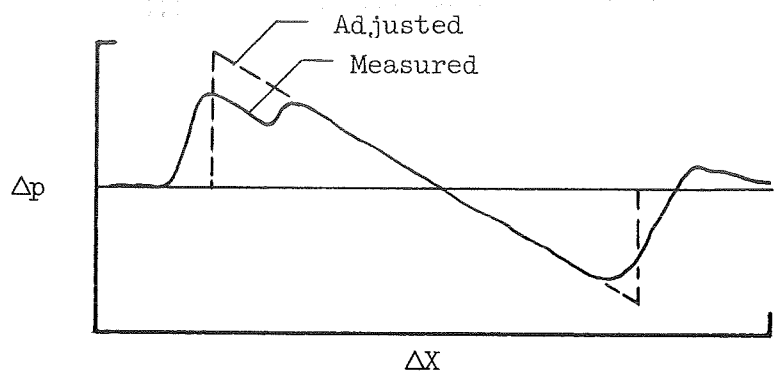

Sketch 1

In order to study the influence of vibration, consider a completely steady model in uniform supersonic flow and an ideal pressure sensing system with a probe at a distance large enough so that a true far-field N-wave is recorded, as represented by the long-dash line in sketch 2. Suppose that the model (or the

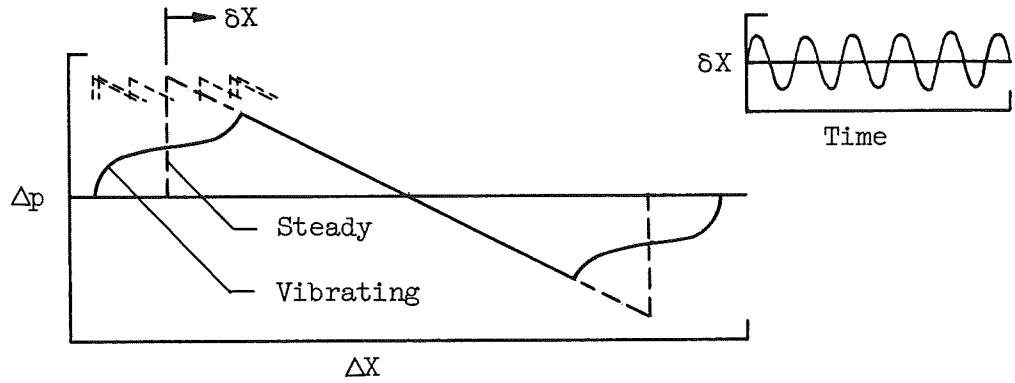

Sketch 2

measuring probe) undergoes a constant-amplitude vibratory motion represented by the inset sketch in sketch 2. In this case, the N-wave will occupy successive positions at equal time increments as indicated by the short-dash lines on the pressure signature plot of sketch 2. At a given longitudinal probe location a highly damped measuring system such as the one used for these tests would register a time average of the pressures imposed on it. When a range of probe locations is considered, the measured pressure signature with a constant-amplitude vibrating system takes on the appearance of the solid curve. This curve does not resemble the actual wind-tunnel data, but it is not likely that tunnel vibration is confined to the single amplitude shown here.

When a varying amplitude is considered, the resulting pressure signature assumes the characteristics of that shown in sketch 3. The assumed amplitude-time relationship is shown in the inset. The resulting signature now resembles those obtained from actual tunnel measurements.

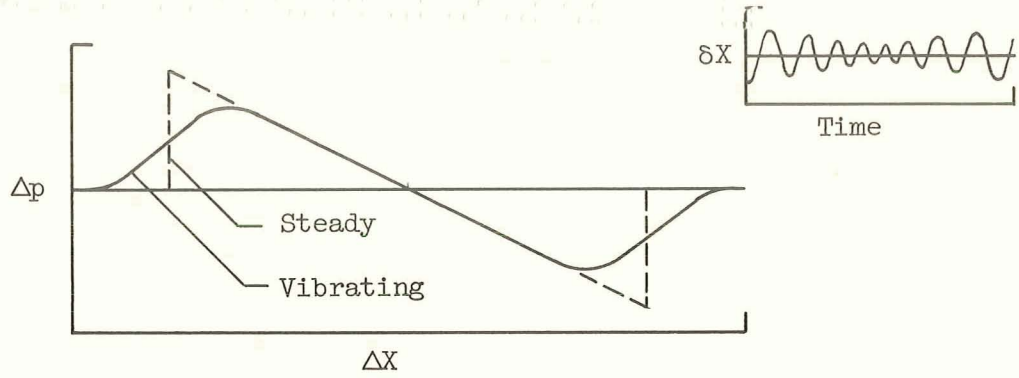

Sketch 3

In both sketches 2 and 3, note that the areas under the curves are almost unchanged from the steady to the vibrating condition. Also note that the middle portion of the signature remains unaffected provided the amplitude of the vibration is less than the length of the signature. These observations may now be utilized in an attempt to adjust the measured data to provide an estimate of the pressure signature in the absence of vibration. This adjustment may be accomplished by extending the linear portion of the measured signature forward so that a right triangle is formed whose area is equal to the area under the measured curve. Since this procedure is identical to that previously discussed in the compensation for the presence of near-field pressure signature characteristics, one adjustment will suffice for both deficiencies.

The foregoing discussion of vibration effects was considered to be independent of possible viscous effects. The boundary layer, however, is a significant factor in the sensing of static-pressure changes across shock waves. The imposition of shock-wave pressure gradients on boundary layers of pressure-sensing instruments generally produces flow distortions which can be sensed both upstream and downstream of shock locations. This condition effectively results in tendencies for instrument-sensed pressure changes across shock waves to be less abrupt than pressure discontinuities across the shock waves in the absence of instruments. Such effects of boundary layer, as well as effects of vibration, in spreading and rounding off shock-wave pressure signatures are approximately accounted for by the previously described technique for adjusting wind-tunnel pressure measurements. The applicability of the adjustment technique may be uncertain, however, if the pressure-sensing arrangements are different from those employed in references 4 and 6 and in the present investigation.

The application of this adjustment technique may be observed in the following example. Sketch 4 shows a wind-tunnel measured pressure signature for a model of a supersonic bomber airplane (configuration 2) representative of those obtained in reference 4. An adjusted tunnel pressure signature is obtained by constructing a right triangle having the measured slope and having an area equal to the area under the measured signature. (The method suggested herein yields results similar to those obtained by using the method of ref. 4. However, this proposed adjustment method has the added feature of being applicable to complex

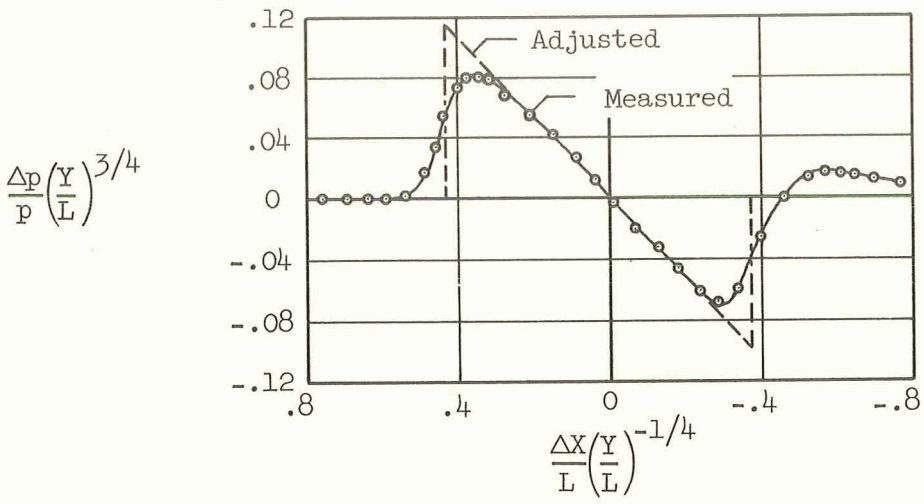

Sketch 4

signatures where near-field phenomena are evident.) In sketch 5 adjusted values of the tunnel measured pressure rise at the bow shock for configuration 2 of reference 4 are compared with theory.

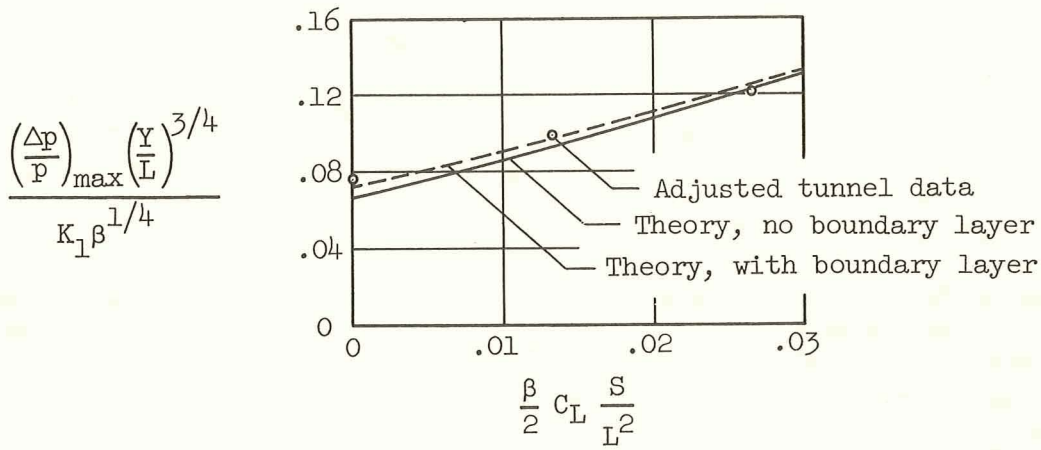

Sketch 5

The measured pressures compare more favorably with the theory when the added thickness of a laminar boundary layer (as discussed in the text) is considered.

In order to indicate the ability of the wind-tunnel data corrected on the basis of this technique to estimate flight results, a comparison of adjusted tunnel data with flight data for a bomber airplane has been made. The extrapolation of adjusted tunnel data to full-scale conditions takes into account differences in the relative thickness of the boundary layer on the model and on the airplane evaluated in the following manner. The theoretical value of sonic-boom

overpressure parameter is obtained for the model by using an area distribution which includes the estimated displacement thickness of a laminar boundary layer and for the airplane by using an area distribution which includes the estimated displacement thickness of a turbulent boundary layer. The difference in these theoretical values is then subtracted from a fairing of experimental data as presented in sketch 5. This revised curve, together with the appropriate values for the factors in the overpressure and lift parameters may then be used in estimating the ground overpressure.

For the range of flight conditions (altitude, Mach number, and weight) covered in reference 8, sketch 6 shows a comparison of measured pressure on the ground directly below the airplane with estimates based on tunnel data and with theory. In both the theory and tunnel data estimates, the reference pressure p

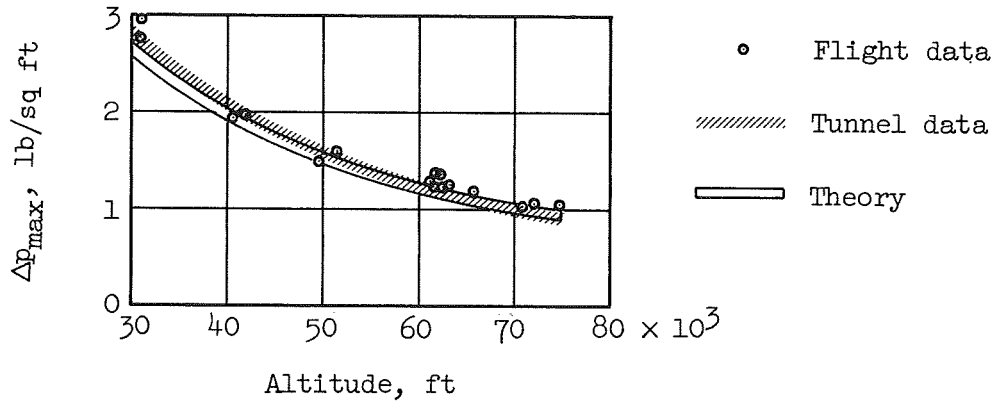

Sketch 6

was taken as the pressure at mid-altitude and the reflection factor for the dry lake bed over which the flights were made was chosen as 2.0. The reasonably close agreement of flight data, adjusted tunnel data, and theory may be taken as an indication of the degree of confidence which may be placed on further estimates made by using these methods.

REFERENCES

1. Spearman, M. Leroy, Driver, Cornelius, and Robins, A. Warner: Aerodynamic Characteristics at Mach Numbers of 2.30, 2.96, and 3.50 of a Supersonic Transport Model With a Blended Wing-Body, Variable-Sweep Auxiliary Wing Panels, and Outboard Tail Surfaces. NASA TM X-803, 1963.

2. Whitcomb, Richard T., Patterson, James C., Jr., and Kelly, Thomas C.: An Investigation of the Subsonic, Transonic, and Supersonic Aerodynamic Characteristics of a Proposed Arrow-Wing Transport Airplane Configuration. NASA TM X-800, 1963.

3. Carraway, Ausley B., Morris, Owen G., and Carmel, Melvin M.: Aerodynamic Characteristics at Mach Numbers From 0.20 to 4.63 of a Canard-Type Supersonic Commercial Air Transport Configuration. NASA TM X-628, 1962.

4. Carlson, Harry W.: Wind-Tunnel Measurements of the Sonic-Boom Characteristics of a Supersonic Bomber Model and a Correlation With Flight-Test Ground Measurements. NASA TM X-700, 1962.

5. Walkden, F.: The Shock Pattern of a Wing-Body Combination, Far From the Flight Path. Aero. Quarterly, vol. IX, pt. 2, May 1958, pp. 164-194.

6. Carlson, Harry W.: An Investigation of the Influence of Lift on Sonic-Boom Intensity by Means of Wind-Tunnel Measurements of the Pressure Fields of Several Wing-Body Combinations at a Mach Number of 2.01. NASA TN D-881, 1961.

7. Carlson, Harry W.: The Lower Bound of Attainable Sonic-Boom Overpressure and Design Methods of Approaching This Limit. NASA TN D-1494, 1962.

8. Hubbard, Harvey H., Maglieri, Domenic J., Huckel, Vera, and Hilton, David A.: Ground Measurements of Sonic-Boom Pressures for the Altitude Range of 10,000 to 75,000 Feet. NASA TM X-633, 1962.

9. Friedman, Manfred P.: Sonic Boom Studies. Tech. Rep. 29, Aerophysics Lab., M.I.T., Feb. 1962.

10. Lina, Lindsay J., and Maglieri, Domenic J.: Ground Measurements of Airplane Shock-Wave Noise at Mach Numbers to 2.0 and at Altitudes to 60,000 Feet. NASA TN D-235, 1960.

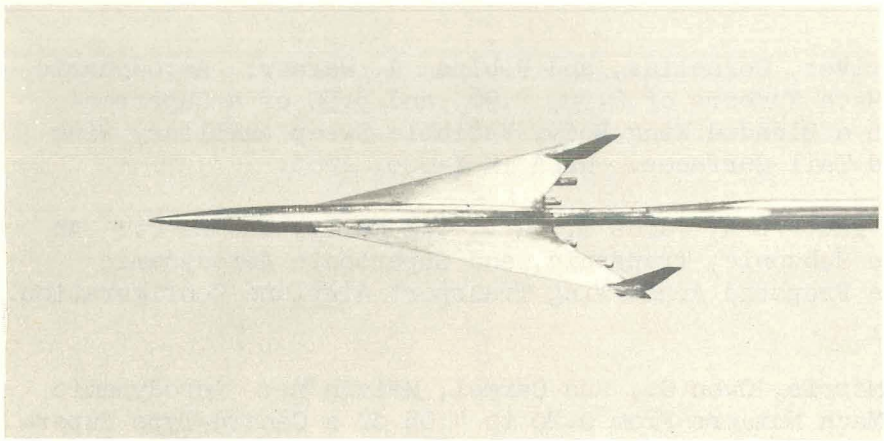

Configuration 1

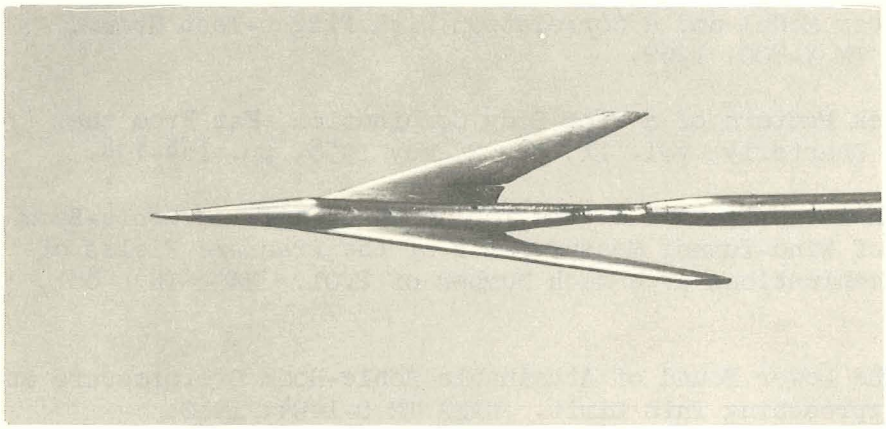

Configuration 2

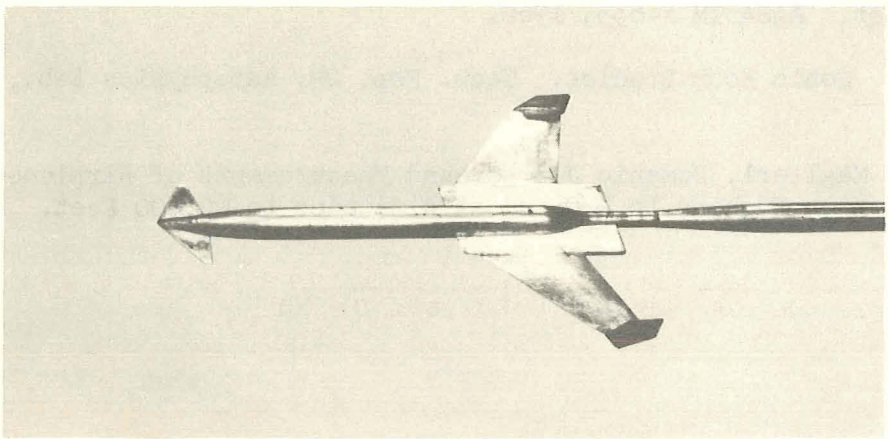

Configuration 3

Figure 1.- Photographs of models. L-63-3194

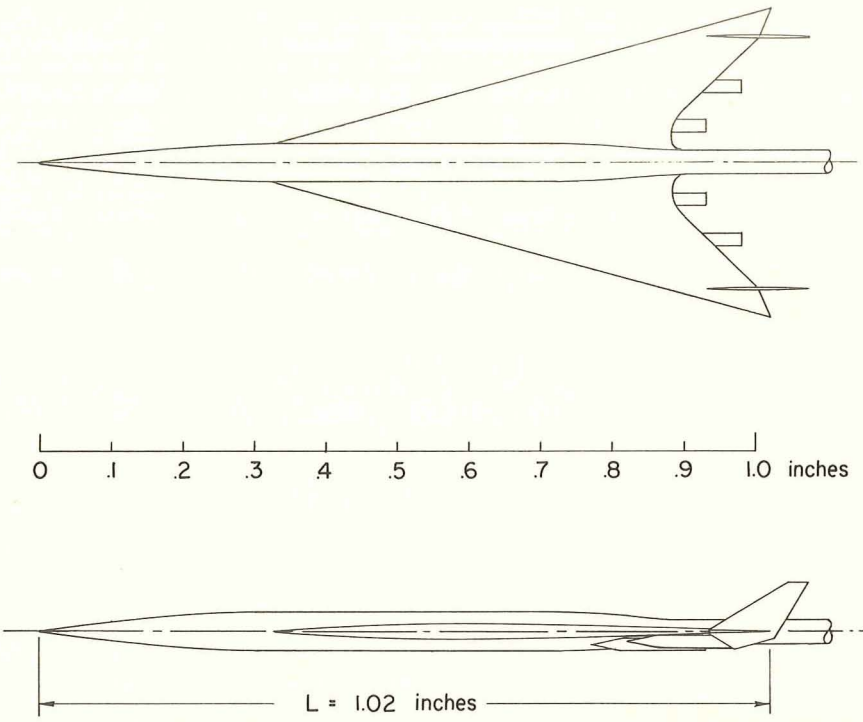

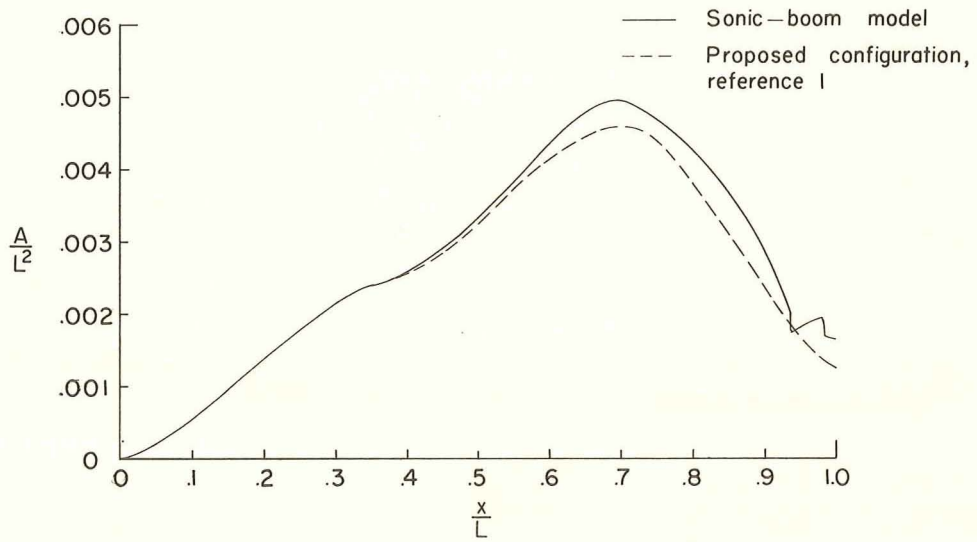

(a) Configuration 1.

Figure 2.- Sketches of models.

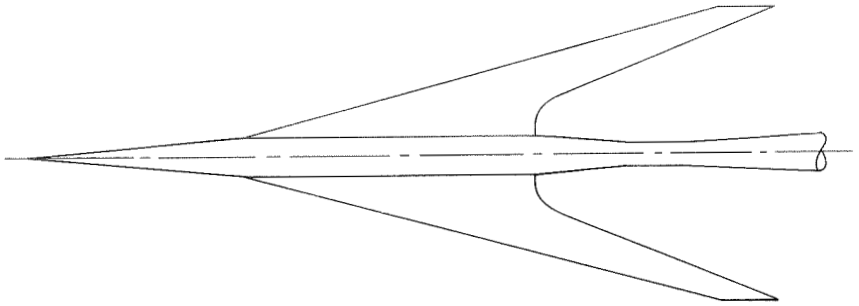

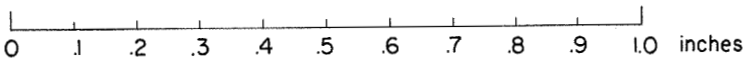

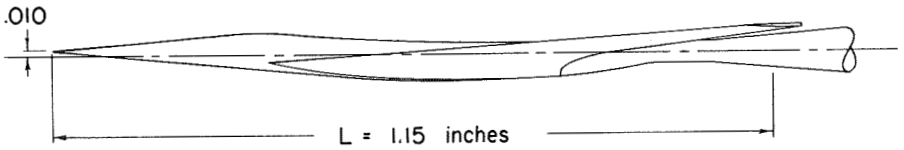

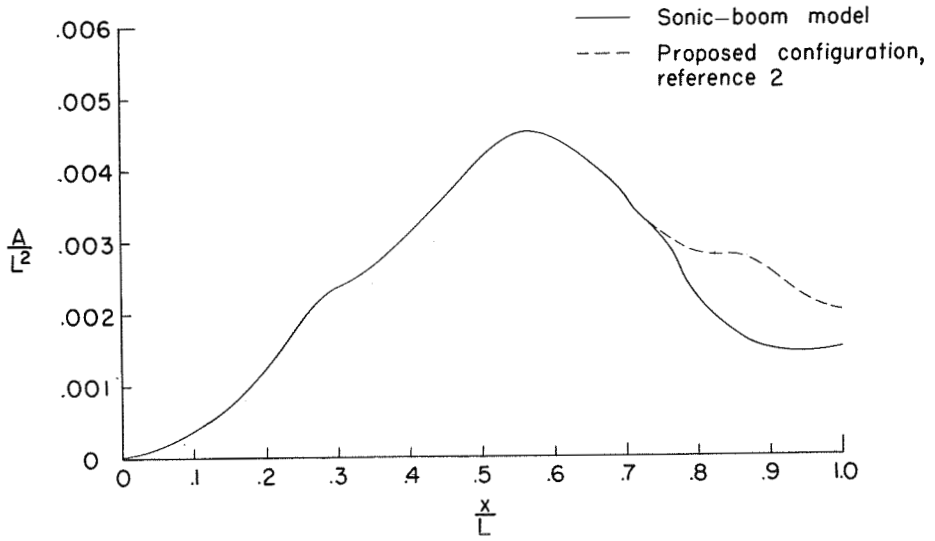

(b) Configuration 2.

Figure 2.- Continued.

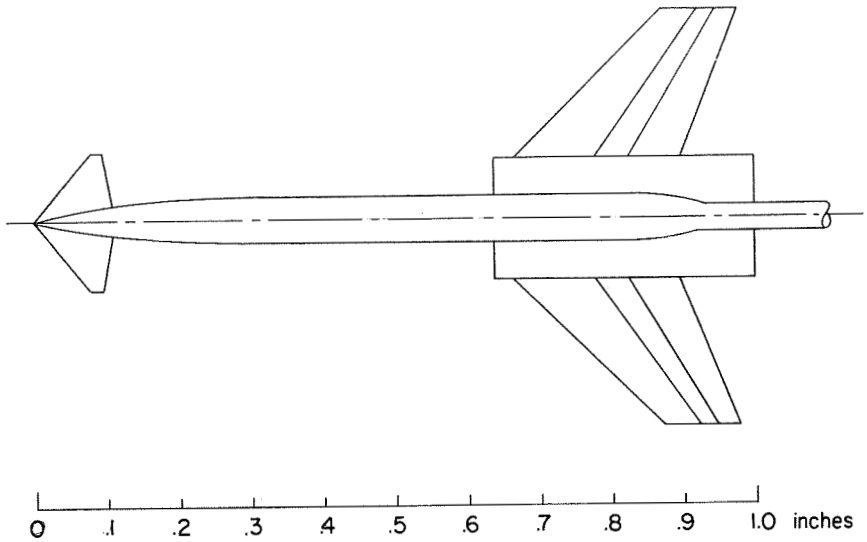

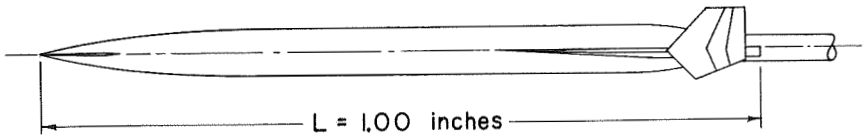

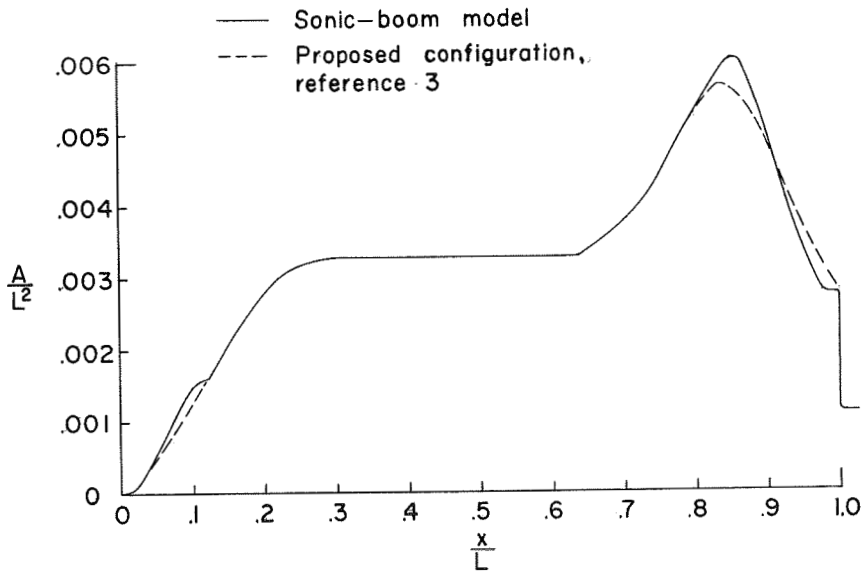

(c) Configuration 3.

Figure 2.- Concluded.

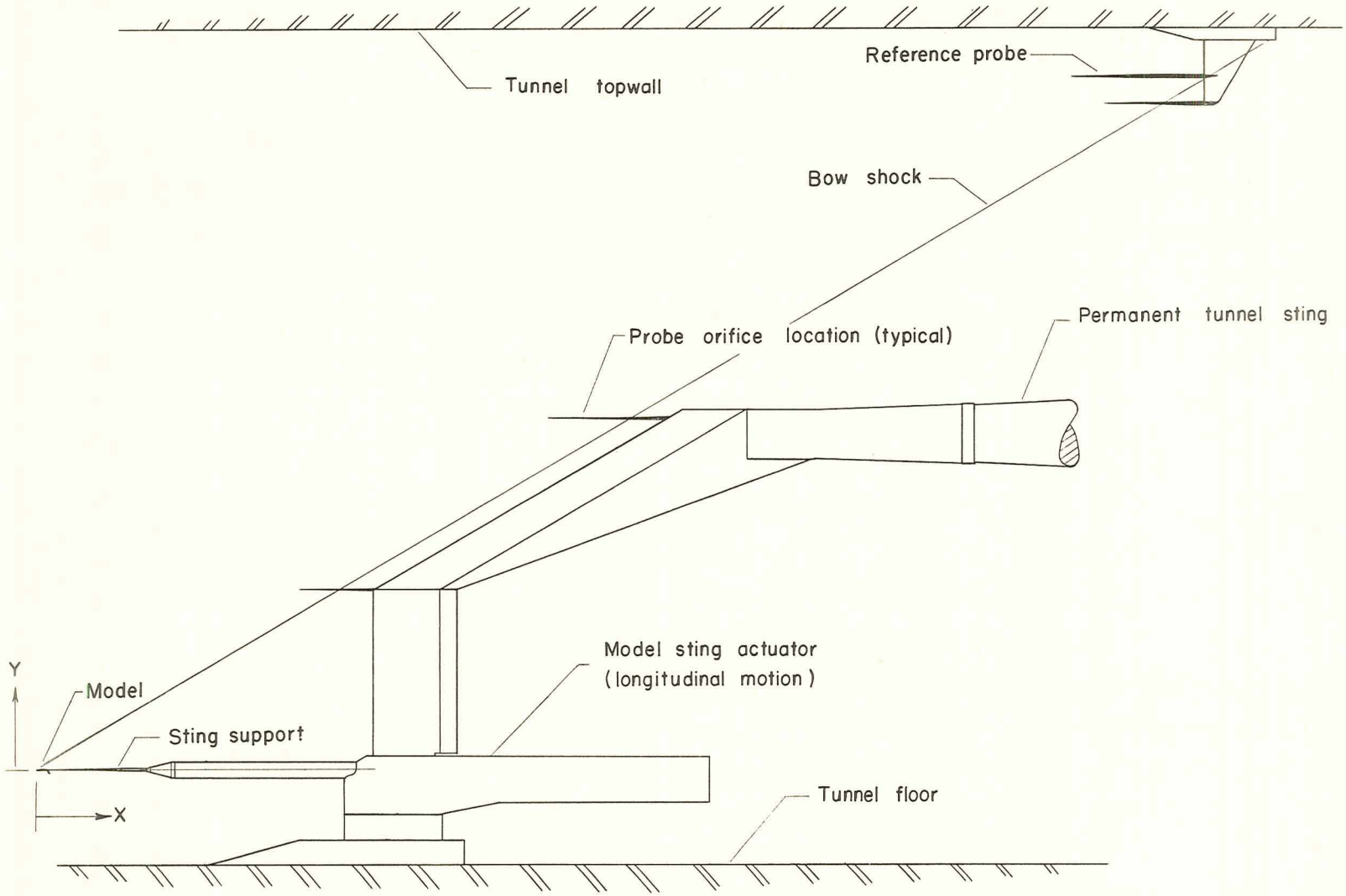

Figure 3.- Sketch of test setup.

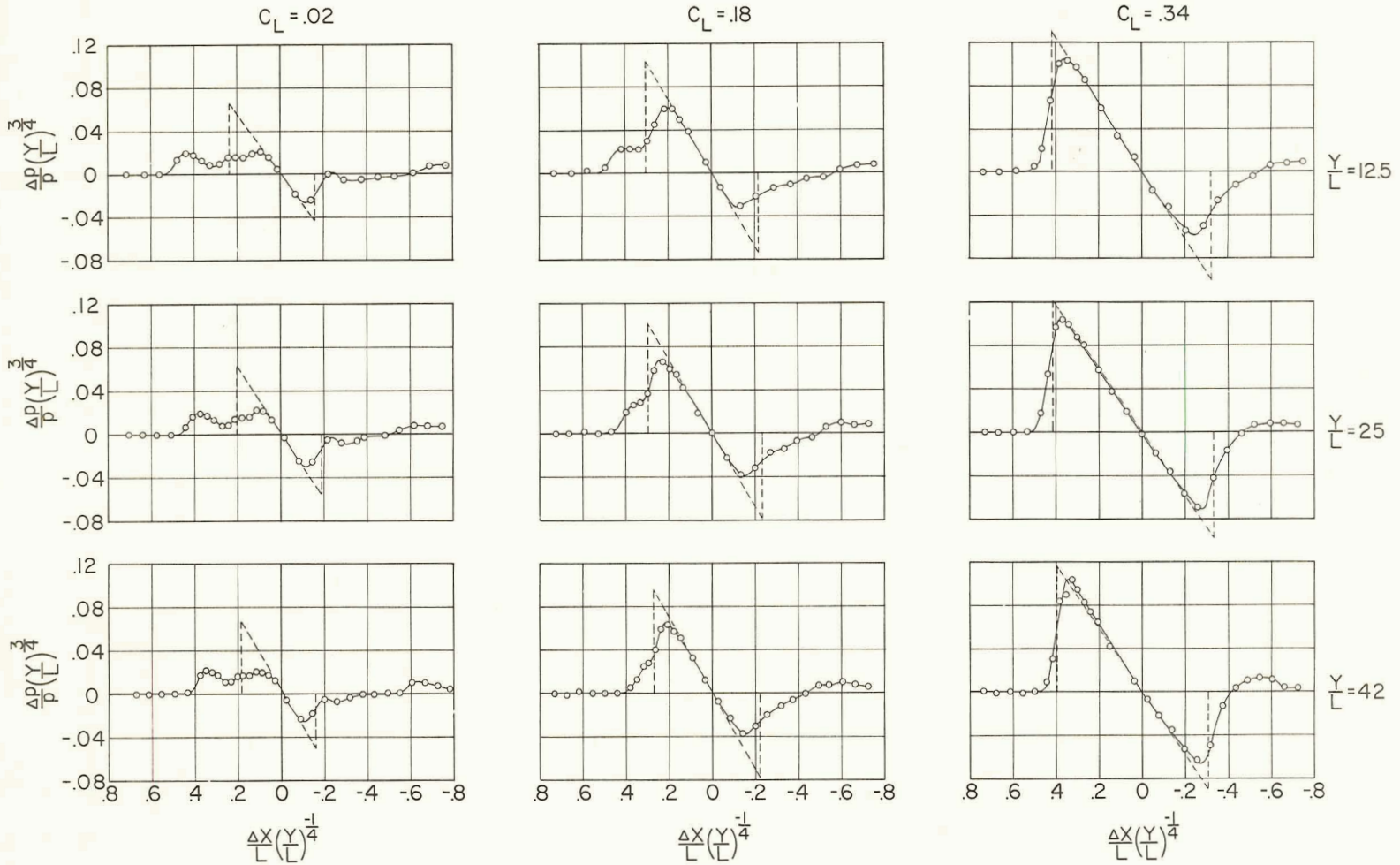

(a) Configuration 1; M = 1.41.

Figure 4.- Measured pressure signatures. Dashed line indicates adjusted signature.

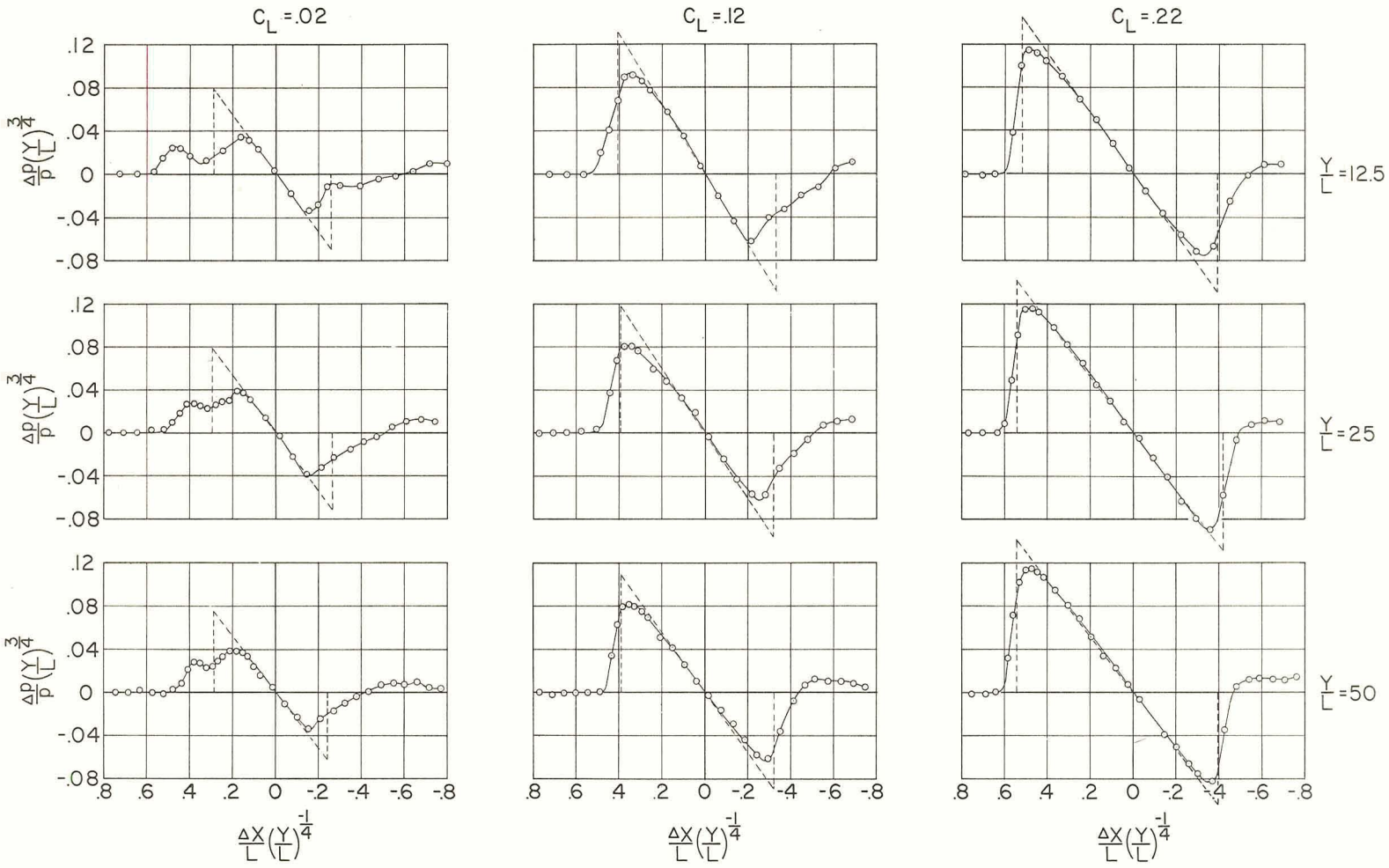

(b) Configuration 1; M = 2.01.

Figure 4.- Continued.

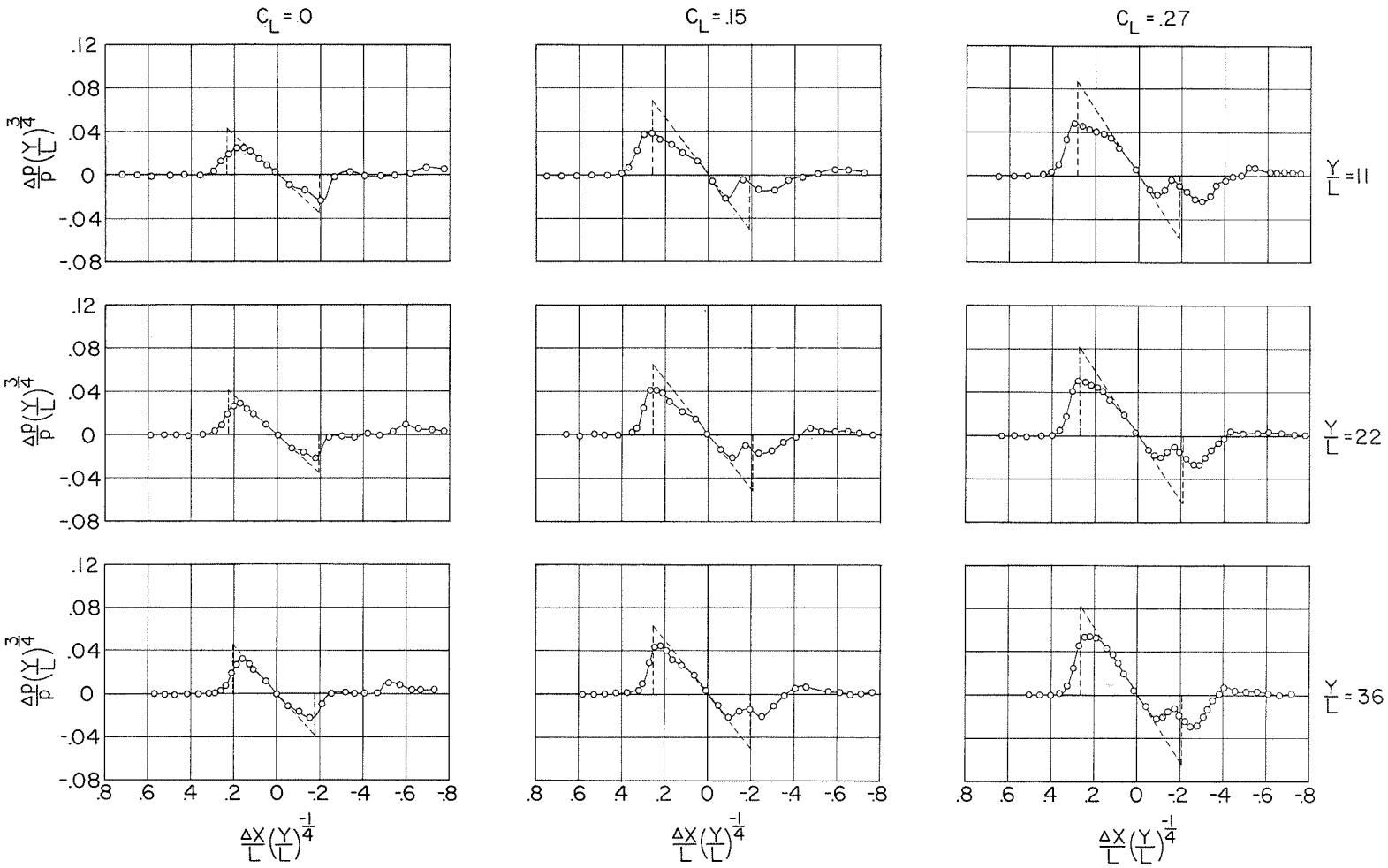

(c) Configuration 2; M = 1.41.

Figure 4.- Continued.

(d) Configuration 2; M = 2.01.

Figure 4.- Continued.

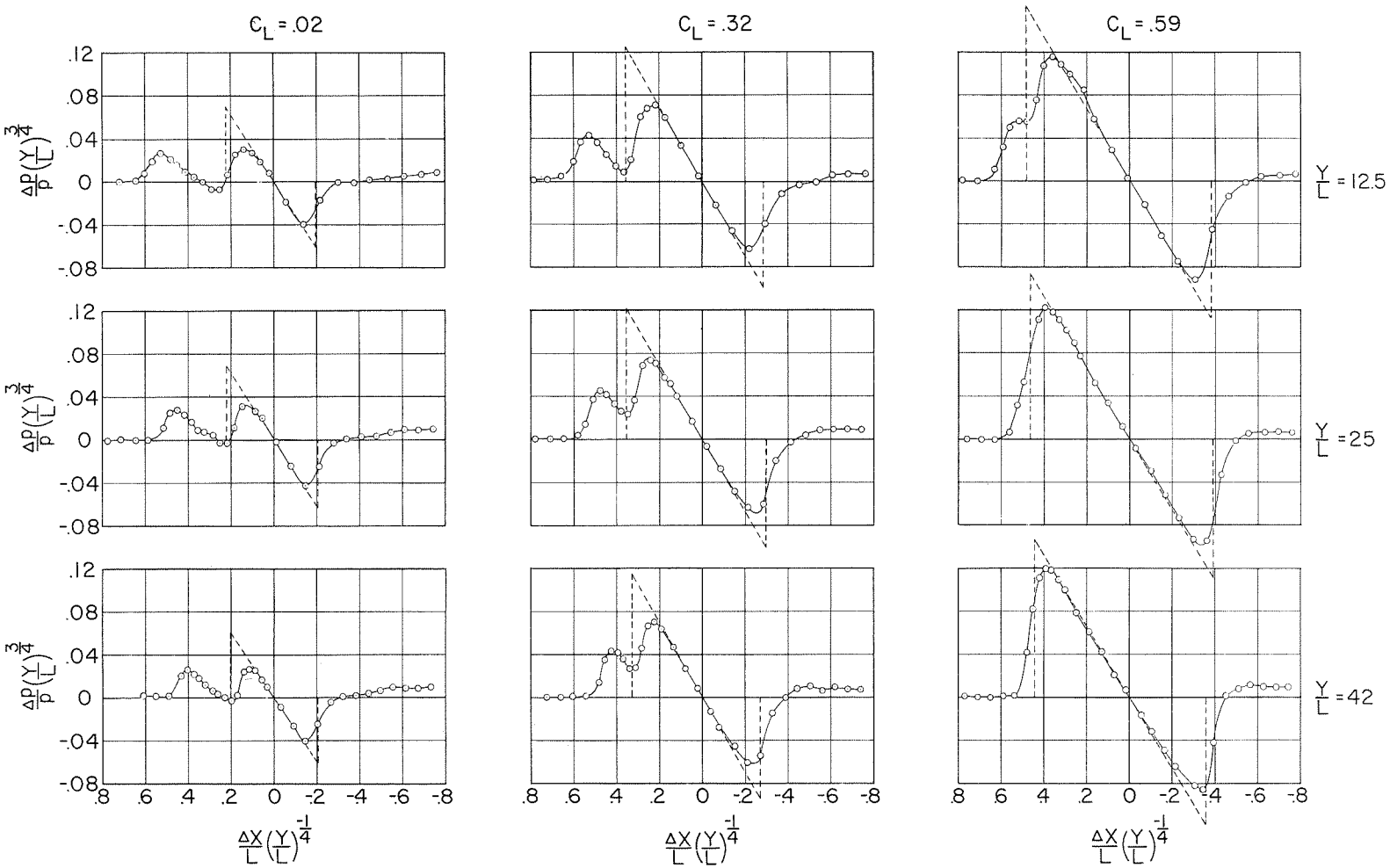

(e) Configuration 3; M = 1.41.

Figure 4.- Continued.

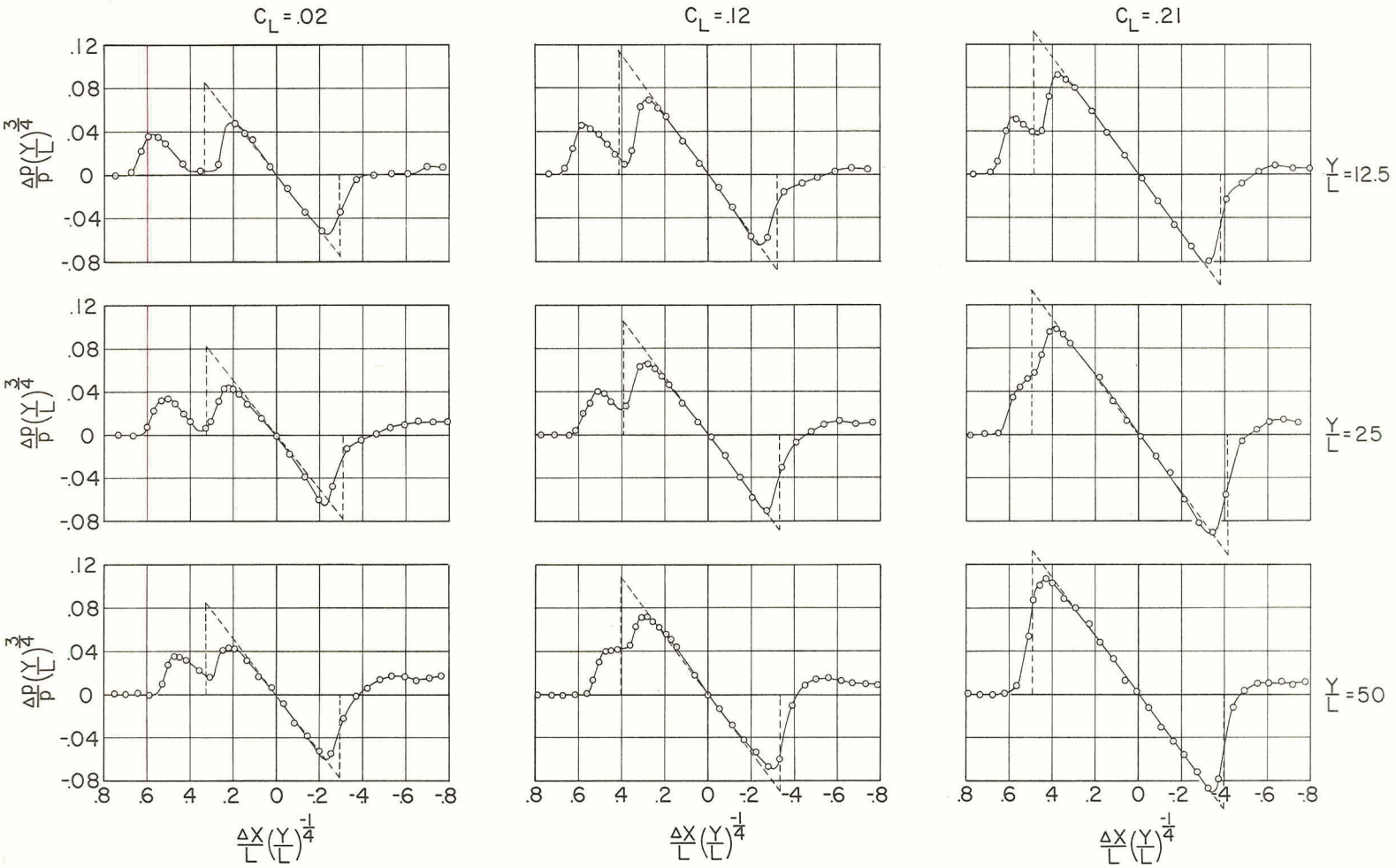

(f) Configuration 3; M = 2.01.

Figure 4.- Concluded.

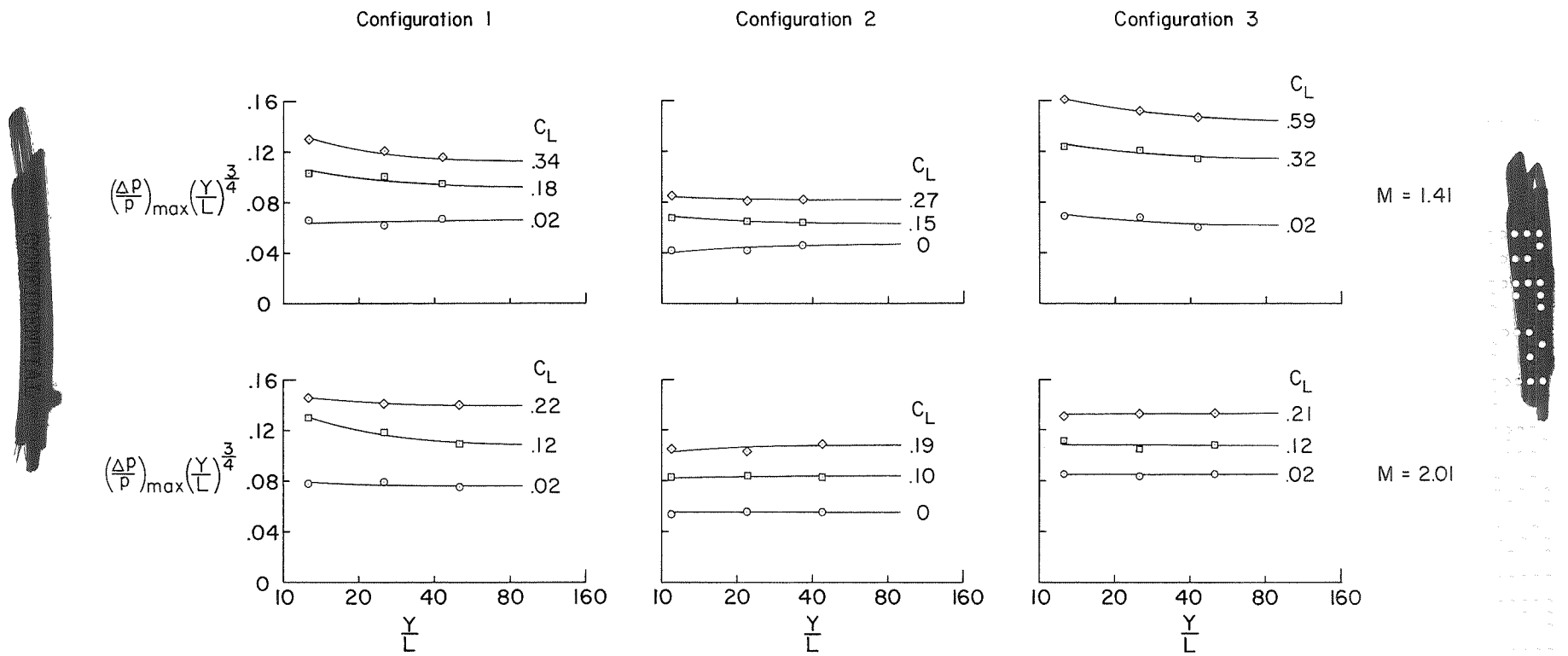

Figure 5.- Variation of adjusted bow-shock pressure rise with distance.

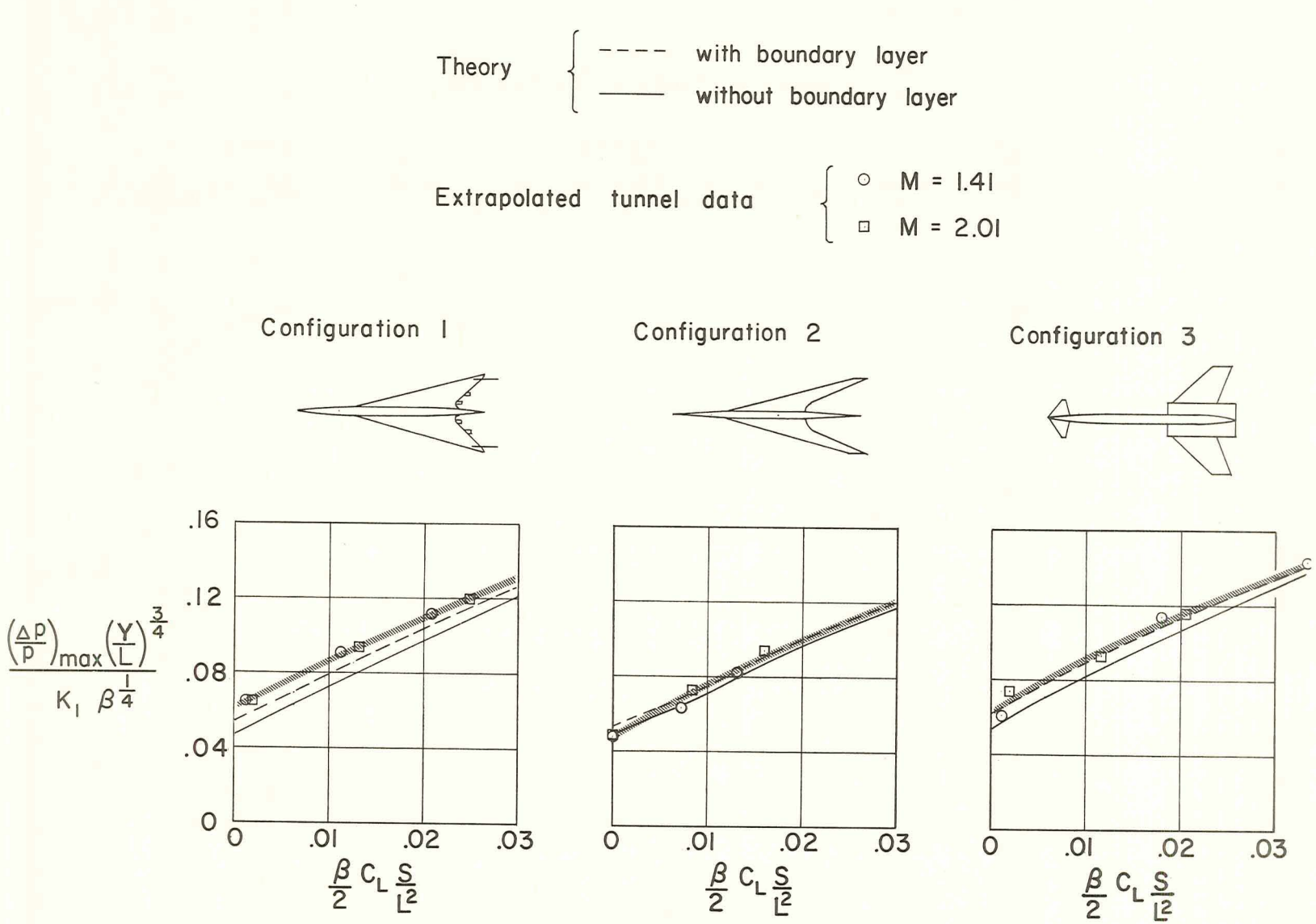

Figure 6.- Comparison of extrapolated tunnel data with theory.

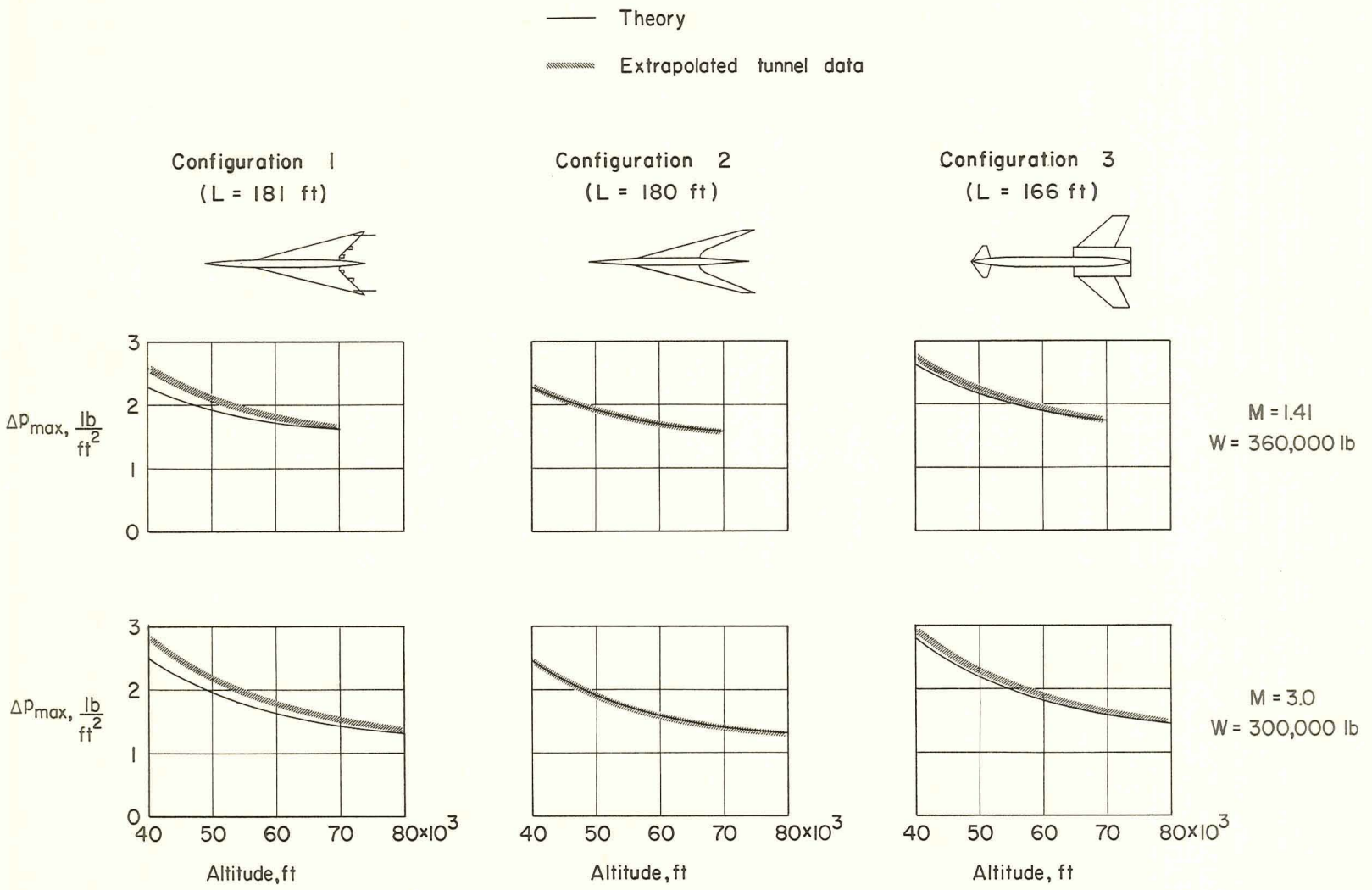

Figure 7.- Estimated ground overpressures.